A generalised approach to rapid finite element design of notched materials against static loading using the Theory of Critical Distances

R. Louks, H. Askes, L. Susmel
Department of Civil and Structural Engineering, The University of Sheffield,
Sheffield S1 3JD, United Kingdom

Corresponding Author: Prof. **Luca Susmel**
Department of Civil and Structural Engineering
The University of Sheffield, Mappin Street, Sheffield, S1 3JD, UK
Telephone: +44 (0) 114 222 5073
Fax: +44 (0) 114 222 5700
e-mail: l.susmel@sheffield.ac.uk

Abstract

The aim of this paper is promoting a simple approach whose use - together with conventional linear-elastic Finite Element (FE) analysis - results in estimates that are more accurate than those obtained by applying the classic Hot-Spot Stress Method. The generalised formulation of the Theory of Critical Distances (TCD) being proposed calculates the required critical distance from two readily available material properties, namely, the ultimate tensile strength, and the plane strain fracture toughness. This alleviates the need for further testing normally required in the conventional TCD methods which can be costly. An extensive search through the technical literature has resulted in a data base storing approximately 800 experimental results, which have been used to validate this simplified TCD methodology. The investigated test samples contained a range of notch root radii from 0.01mm up to 7mm. The specimens were made of a variety of engineering materials, exhibiting brittle, quasi-brittle and ductile mechanical behaviour, and were tested under uniaxial as well as multiaxial static loading. This extensive validation exercise demonstrates that the proposed simplified methodology is a powerful engineering tool which allows static strength to be estimated more accurately than with the classic Hot-Spot Stress Method.

Keywords: Theory of Critical Distances, Static fracture, Notches, Design, Mixed-Mode loading

Nomenclature

E	Error [%]
E_{max}	maximum error
E_{min}	minimum error (critical error)
E_a	average error
$\Delta E=E_{max}-E_{min}$	error range
K_{IC}	plain strain fracture toughness

L	critical distance
L_E	engineering critical distance
Oxyz	system of coordinates
Orθ	polar system of coordinates
S_F	safety factor
ρ	notch root radius
σ_{eff}	effective stress
σ_{eq}	equivalent stress
$\sigma_{HS,eq}$	equivalent stress at the hot spot
σ_n	maximum normal stress
σ_{nom}	nominal stress
σ_{UTS}	ultimate tensile strength
σ_{VM}	Von Mises equivalent stress
σ_x, σ_y	normal stress components
σ_o	material inherent strength
σ_1	maximum principal stress
τ_{xy}	shear stress component

1. Introduction

The geometry of structural components is often such that notches or keyways are inevitable, thus raising the magnitude of the local stresses. Accurately predicting the failure of engineering materials experiencing localised stress concentration phenomena has been the goal of many investigations during the last century, as improved accuracy leads to less unexpected failures and a more efficient usage of natural resources.

Classic brittle materials exhibit a perfectly elastic stress-strain curve up to failure. On the contrary, un-notched ductile polymers and metals will deviate from the elastic behaviour, showing some plasticity prior to failure. In the presence of stress concentration features, engineering materials can fail by different mechanisms compared to those acting in the absence of notches: for instance, the presence of a sharp notch may promote brittle fast fracture also in those materials which are relatively ductile in their plain form [1]. Thus, accurately estimating the static strength of notched components is not straightforward.

In situations of practical interest components are often designed via the Hot-Spot Stress Method (HSSM) which is known to be very conservative when it is used to assess the detrimental effect of finite radius stress concentrators [2]. However, this design methodology is quick and simple to implement, making it attractive in those situations where time and costs are crucial factors. In particular, the HSSM is usually applied by recording the surface results from conventional linear-elastic Finite Element (FE) models, with the stress state at that material point experiencing the largest magnitude of the stress being used to determine the corresponding safety factor.

Examination of the state of the art suggests that the so-called Theory of Critical Distances (TCD) [2] represents an interesting alternative to the classic HSSM. In particular, the TCD has been demonstrated to be successful in predicting the static strength of engineering components containing stress concentrators of all kinds and manufactured from materials that exhibit either a brittle, quasi-brittle or ductile mechanical behaviour [3-8]. Systematic application of the TCD was seen to return predictions typically falling within an error interval of ±20% [2].

The TCD requires two additional material properties (i.e., a material length scale parameter denoted as the "critical distance", and an inherent strength) which have to be determined by carrying out expensive and time consuming experiments [6-8]. The reformulation of the TCD presented in this paper aims to eliminate the need for additional testing, this allowing the time and costs associated with the design process to be reduced remarkably. In particular, since engineering materials' manufacturers typically provide end-users with the ultimate tensile strength (UTS, σ_{UTS}) and the plane-strain fracture toughness (K_{IC}), the proposed reformulation of the TCD makes use of these two material properties to directly calculate the required critical distance. The accuracy and reliability of the proposed simplified approach will be checked against a large number of experimental data taken from the literature which was generated by testing brittle, quasi-brittle, and metallic notched materials, the TCD being applied in the form of the Point Method (PM).

2. Review of the TCD

The TCD is a group of theories which use a common critical distance, denoted as L, to assess local linear-elastic stresses ahead of stress concentrator apices. The TCD has been formalised into four methods which include the Point Method (PM), the Line Method (LM), the Area Method, and the Volume Method [2]. Although there are four strategies to apply the TCD, the present investigation will only consider the PM, as the intention is to promote a simple and efficient alternative design solution to the commonly used HSSM (especially when the static assessment is performed by post-processing linear-elastic stress fields determined via conventional linear-elastic FE models).

Critical distance analysis was originally proposed in the 1950s by Neuber [9] who developed a high-cycle fatigue assessment methodology based on the LM idea. In particular, Neuber's approach uses the elastic stress averaged over a material dependent length taken ahead of the assessed stress raising features. Subsequently, Peterson [10] proposed an alternative simplified solution which introduced the PM concept. Peterson's technique assumes that a notched component would fail in the high-cycle fatigue regime when the elastic stress at a material dependent distance from the apex of the assessed stress concentrator reaches a critical stress level.

Later the critical distance analysis was adapted to predict static fracture in a range of materials exhibiting both ductile and brittle mechanical behaviour. In 1974, Whitney and Nuismer [11] investigated the problem of monotonic failure of fibre composite materials containing stress concentration features. With no reported knowledge of the early work, they developed identical theories to the LM and PM but gave them different names. During their investigation they made the useful link between Continuum Mechanics and Linear Elastic Fracture Mechanics (LEFM) allowing them to express the critical distance, L, as a function of the plane-strain fracture toughness, K_{IC}, i.e. [2, 11]:

$$L = \frac{1}{\pi}\left(\frac{K_{IC}}{\sigma_0}\right)^2 \quad (1)$$

In definition (1) σ_o is the so-called material inherent strength whose value depends on the mechanical/cracking behaviour displayed by the material being assessed [2].

Before considering in detail the problem of determining σ_o, it is worth observing here that the TCD has proven to be highly accurate in estimating static strength of notched material by simply post-processing the linear-elastic stress fields acting on the material in the vicinity of the assumed crack initiation locations [3-8]. In other words, accurate predictions can be made by employing a simple linear-elastic constitutive law to model the mechanical behaviour of engineering materials independently from the level of ductility/brittleness. As far as high-cycle fatigue of notched metals is concerned, this simplifying hypothesis is acceptable since in the long-life regime the contribution of plasticity is so much reduced and confined that material non-linearities can be neglected with negligible loss of accuracy [12]. In a similar way, brittle notched materials can accurately be designed against static loading according to the TCD by directly post-processing the local linear-elastic stress fields. Conversely, when the TCD is employed to perform the static assessment of notched ductile materials, accurate estimates can be obtained by adopting a simple linear-elastic constitutive law provided that the material inherent strength σ_o is determined accordingly (and σ_o may then differ significantly from the UTS) [7, 9].

By taking as a starting point his earlier work on ceramics [3], Taylor observed that for brittle engineering materials the inherent strength, σ_o, can be taken equal to the material UTS, σ_{UTS}. This finding is in agreement with Whitney and Nuismer's work [11] which used the UTS as σ_o for some quasi-brittle composite materials successfully. On the contrary, it has been demonstrated that adopting $\sigma_o=\sigma_{UTS}$ to calculate the critical distance does not return accurate results when assessing materials that exhibit, prior to failure, some degree of plasticity in the vicinity of the stress raiser apex (such as, for instance, aluminium [8] and PMMA tested at room temperature [4]). In particular, it has been demonstrated [2, 8] that σ_o becomes larger than σ_{UTS} when final breakage is preceded by large-scale plastic deformations (with this holding true especially in ductile materials exhibiting significant strain hardening [2]). Therefore, as it will be discussed in detail below, the only way to determine the critical distance value for ductile materials is by estimating L from experimental results generated by testing notches of different sharpness. Another important aspect is that the TCD cannot obviously be used to design un-notched ductile materials if $\sigma_o>\sigma_{UTS}$, as this would predict failures with large non-conservative errors [2].

In order to understand the way the TCD works under Mode I loading, consider the uniaxially loaded notched plate sketched in Figure 1a. The TCD postulates that the component being assessed breaks statically as soon as an effective stress, σ_{eff}, determined by post-processing the local linear-elastic stress field becomes equal to the inherent material strength, σ_o [2]. According to the PM, the effective stress is equal to the local stress determined at a distance from the notch tip equal to L/2, i.e. [2, 10] (see also Fig. 1b):

$$\sigma_{eff} = \sigma_y\left(\theta = 0, r = \frac{L}{2}\right) \tag{2}$$

The LM postulates instead that σ_{eff} has to be determined by averaging the linear stress over a distance equal to 2L, i.e. [2, 9] (see also Fig. 1c):

$$\sigma_{eff} = \frac{1}{2L}\int_0^{2L} \sigma_y(\theta = 0, r) \cdot dr \tag{3}$$

As mentioned earlier, as far as brittle materials are concerned, the critical distance L can directly be estimated according to definition (1) by simply taking $\sigma_o=\sigma_{UTS}$ [2]. On the contrary, when final breakage is preceded by local plastic deformations, both σ_o and L have to be determined experimentally by testing samples containing notches of different sharpness. As shown in Figure 2, by plotting, in the incipient failure condition, the linear-elastic stress-distance curve for a sharp as well as for a blunt notch, the TCD material properties can directly be obtained via the coordinates of the point at which the two stress-distance curves cross each other.

The TCD has also proven to be highly accurate in estimating static strength of notched brittle/ductile materials subjected to multiaxial loading [6, 8]. Under mixed mode loading, the orientation of the focus path to be used to determine the necessary stress-distance curve depends on the mechanical/cracking behaviour displayed by the material being assessed. In particular, as far as brittle materials are concerned, the focus path is that straight line (emanating from the assumed crack initiation point) which experiences the largest value of the stress perpendicular to the path itself, σ_n [6] (Fig. 3a). Under these circumstances, the TCD is applied in terms of maximum normal stress, σ_n, and the inherent strength σ_o is suggested as being taken invariably equal to σ_{UTS}. Further, for a specific material, the critical distance value may vary as the degree of multiaxiality of the applied loading changes [6]. This can be ascribed to the fact that a change in the complexity of local stress fields may promote different and more complex fracture mechanisms [6].

Turning to ductile metals [8], the focus path emanates from the assumed crack initiation location and it is perpendicular, at the crack initiation point itself, to the component surface (Fig. 3b). In this case, the highest level of accuracy in designing notched ductile metals is seen to be reached when the TCD is applied by calculating the required equivalent stress, σ_{eq}, according to either von Mises' or Tresca's hypothesis [8, 13].

The literature review of the TCD above shows that, whilst the TCD is an accurate and reliable design tool, its usage in situations of practical interest is not a simple task, to make the most of this powerful theory requires the structural engineer using it to be well trained. Further, in order to minimise the usage of material by systematically reaching an adequate level of safety, the TCD's material properties (i.e., L and σ_o) should always be determined by running appropriate experiments [2], this being sometimes impossible due to a lack of time and resources. In this challenging scenario, the present paper aims to formalise and validate a simplified automated procedure suitable for using the TCD to design notched engineering materials against uniaxial/multiaxial static loading by directly post-processing the results from linear-elastic FE models.

3. Simplified reformulation of the Point Method

As briefly summarised in the previous section, in order to apply the TCD to perform the static assessment of notched components, the first problem to be addressed is the correct determination of both critical distance L and inherent material strength σ_o. If these two material properties cannot be determined by running appropriate experiments, the hypotheses can be formed that, independently from the level of ductility/brittleness characterising the material being designed, σ_o is invariably equal to σ_{UTS}. Therefore, according to definition (1), the corresponding critical distance value can directly be determined as follows:

$$L_E = \frac{1}{\pi}\left(\frac{K_{IC}}{\sigma_{UTS}}\right)^2 \tag{4}$$

This engineering definition for the TCD critical distance is clearly very convenient since manufacturers typically provide σ_{UTS} and K_{IC}.

The second problem to be addressed is the definition of a simple geometrical rule suitable for efficiently defining the origin and orientation of the focus paths. It is commonly accepted that the static fracture processes resulting in component failure take place in the highly stressed regions. Accordingly, those superficial points experiencing the largest stress can be taken as the starting points of the focus paths which continue perpendicular from the surface itself (Fig. 4). The advantage of this simple rule is that it can be applied automatically to post-process linear-elastic stress fields determined via commercial FE software packages. Further, under complex multiaxial loading, the linear-elastic hot-spot stress in the notch root moves as the degree of multiaxiality of the applied loading varies. Therefore, the simple rule proposed above allows origin and orientation of the focus paths to be determined unambiguously and independently from the component geometry and the applied system of loads.

It is common practise to design brittle materials against static loading by using the so-called maximum principal stress criterion. On the contrary, the static assessment of ductile metals is usually performed in terms of von Mises equivalent stress. Therefore, in the present paper it is proposed to apply the TCD either in terms of maximum principal stress, σ_1, or in terms of von Mises stress, σ_{VM}.

According to the simple geometrical rule for the determination of the focus path sketched in Figure 4, the PM can then be rewritten as follows:

$$\sigma_{eff} = \sigma_{eq}\left(r = \frac{L_E}{2}\right) \tag{5}$$

In this definition for the effective stress, σ_{eff}, critical distance L_E is calculated according to Eq. (4), whereas the equivalent stress σ_{eq} can be taken equal to either σ_1 or σ_{VM}, as discussed above (Fig. 4).

As far as notched brittle materials subjected to Mode I loading are concerned, the use of the TCD is expected to result in its usual level of accuracy since $\sigma_o=\sigma_{UTS}$ leads to $L=L_E$. On the contrary, nothing can be said *a priori* about the accuracy of the proposed simplified approach when it is employed to perform the static assessment under multiaxial loading. In fact, whilst the critical distance value has been shown to change as the degree of multiaxiality of the applied loading varies [6], in the present investigation the hypothesis is formed that the TCD length scale parameter is constant and invariably equal to L_E. Further, the focus path determined according to the geometrical rule shown in Figure 4 may be different from the one recommended to be used to design notched brittle components against multiaxial static loading (i.e., it may be different from that path experiencing the maximum opening stress) [6].

Turning to ductile notched materials, the most critical issue associated with the proposed simplified methodology is that engineering critical distance L_E is suggested as being estimated by taking σ_o invariably equal to σ_{UTS}. The schematic stress-distance curve plotted, in the incipient failure condition, in Figure 5 shows the way the PM assesses static strength of a notched ductile material when the critical distance is calculated according to definition (1) as well as to definition (4). As briefly recalled earlier, if final breakage is preceded by localised plastic deformations, σ_0 is seen to be larger than σ_{UTS} [2, 6]. This implies that, K_{IC} being constant, the simplified critical distance value, L_E, becomes larger than the corresponding value, L. Further, nothing can be said *a priori* about the accuracy of this simplified version of the PM in assessing the static strength of notched ductile materials subjected to in-service multiaxial loading.

These considerations should make it evident that the only way to answer the above key questions is by checking the accuracy of the simplified reformulation of the PM proposed in the present paper against an appropriate set of experimental data. This will be done next.

4. Validation methodology

A systematic bibliographical investigation was carried out in order to find experimental results suitable for checking the accuracy and reliability of the proposed simplified design methodology. The developed database contained experimental results generated by testing brittle, quasi-brittle, and metallic notched materials under Mode I, Mode II, Mode III, Mixed-Mode I+II, and Mixed-Mode I+III loading. Tables 1 to 3 summarise the investigated materials - classified as brittle, B (Tab. 1), quasi-brittle, QB (Tab. 2), and metallic materials, M (Tab.3), the temperature at which the tests were conducted, the testing set-up, and the material UTS, σ_{UTS}. The sharpness of the stress concentration features are provided, for any material, in the form of minimum and maximum value of the notch root radius, ρ. Finally, for each considered material, critical distance L_E calculated according to definition (4) is reported. The results considered in the present investigation were generated by testing U- and V-notched flat/cylindrical specimens as well as bluntly/sharply notched half- and full-Brazilian disks. The reader is referred to the original bibliographical sources for a detailed description of the considered specimens as well as of the testing methods being used in the different investigations.

The geometries of the analysed specimens were modelled using finite element software ANSYS®. After applying appropriate boundary conditions, the solution for each model was calculated by assuming that the investigated materials were linear-elastic, isotropic and homogeneous. The mesh density in the vicinity of the stress raisers was refined until convergence occurred; typically this was reached by using elements having size equal to about $L_E/20$ in the regions of the notch root. To calculate the local effective stresses, σ_{eff}, according to the simplified version of the PM, Eq. (5), origin and orientation of the used focus paths were systematically determined according to the geometrical rule shown in Figure 4. The required linear-elastic stress-distance curves were initially determined from the solved FE models in terms of σ_1, this being done independently from the level of ductility characterising the investigated material. Subsequently, for the metallic materials, the linear-elastic stress-distance curves were calculated and post-processed also in terms of Von Mises equivalent stress, σ_{VM}. Failure predictions were compared with the experimental results by calculating the error as follows:

$$E = \frac{\sigma_{eff} - \sigma_{UTS}}{\sigma_{UTS}} \ [\%] \qquad (6)$$

The error calculation for each data will show if the proposed method predicts the failure conservatively or non-conservatively by assigning either positive or negative sign, respectively. The obtained estimates were also assessed in terms of safety factor, S_F, that was calculated as follows [38]:

$$S_F = \frac{\sigma_{UTS}}{\sigma_{eff}} \ [\%] \qquad (7)$$

Finally, to assess the competitive performance of the proposed TCD based design methodology, the HSSM was applied consistently to all data as well, by refining the mesh until convergence was reached at the surface. All FE models were post-processed according to the HSSM in terms of σ_1, von Mieses equivalent stress, σ_{VM}, being used solely for the notched metallic materials. To assess the accuracy of the HSSM, errors and safety factors [38] were calculated as follows:

$$E = \frac{\sigma_{HS,eq} - \sigma_{UTS}}{\sigma_{UTS}} \ [\%] \tag{8}$$

$$S_F = \frac{\sigma_{UTS}}{\sigma_{HS,eq}} \tag{9}$$

where $\sigma_{HS,eq}$ is the equivalent stress at the hot spot determined according to either the maximum principal stress criterion, σ_1, or Von Mises criterion, σ_{VM}, as appropriate.

5. Results

The experimental results summarised in Tables 1 to 3 were initially post-processed according to the HSSM. This was done to be able to compare the accuracy of the simplified reformulation of the TCD being proposed to the one obtained by using the classic HSSM (i.e., by applying that approach most commonly used in situations of practical interest to perform the static assessment through the results from linear-elastic FE models [2]).

As far as brittle and quasi-brittle materials are concerned, the error diagrams reported in Figures 6a and 6b show that, independently of the degree of multiaxiality of the applied loading, the use of the HSSM with $\sigma_{HS,eq}=\sigma_1$ resulted in conservative estimates, with the level of conservatism increasing as the notch root radius, ρ, decreases. The average error obtained for brittle materials was equal to 111%, whereas for the quasi-brittle materials it was equal to 171%. For both types of materials, the critical error (defined as the most non-conservative error being recorded) was equal to about -35%.

Turning to the metals being investigated, the HSSM was applied by taking $\sigma_{HS,eq}$ equal to both σ_1 and σ_{VM}. The error charts of Figures 6c and 6d make it evident that the systematic usage of the HSSM resulted in very conservative predictions, with an average error equal to about 450% and a critical error approaching -10%.

The overall accuracy obtained by using the HSSM to post-process the investigated results is summarised in Table 4 in terms of maximum error, E_{max}, minimum error (i.e., critical error), E_{min}, average error, E_a, and error range, $\Delta E=E_{max}-E_{min}$. According to this table, whilst the HSSM is highly conservative with a low critical error (i.e., E_{min} equal to about -10%), its systematic usage resulted in highly scattered predictions with a ΔE value larger than 3500%.

Turning to the simplified TCD, initially the data summarised in Tables 1 to 3 were post processed by taking $\sigma_{eq}=\sigma_1$ in Eq. (5). As far as brittle and quasi-brittle notched materials are concerned, the error diagrams reported in Figures 7a and 7b, respectively, show that the use of the simplified TCD resulted in a much larger degree of accuracy compared to the one obtained by applying the HSSM (see Figures 6a and 6b for comparison). In particular, the proposed simplified methodology was capable of estimates falling within an error range of about 200%. For brittle materials, the critical error was equal to -33%, with an average error of 32%. For quasi-brittle materials, the critical error was seen to be equal to -53% and the average error to 18%.

Focussing attention on the results generated by testing notched metallic materials, the error chart of Figure 7c shows that the use of the TCD along with $\sigma_{eq}=\sigma_1$ resulted in an average error of 12%, the critical error being equal to -70%. More accurate results were obtained by re-analysing this data by taking $\sigma_{eq}=\sigma_{VM}$ in Eq. (5): according to Figure 7d, the use of the TCD with $\sigma_{eq}=\sigma_{VM}$ resulted in an average error of -13%, with the critical error being equal to -49%.

Table 4 allows the TCD to be compared directly to the HSSM. This table confirms that, in terms of error range, the use of the TCD allowed the scattering of the obtained estimates to be reduced by an order of magnitude. However, the intrinsic level of conservatism characterising the HSSM led to critical error values that were lower than the corresponding ones obtained using the TCD (especially for the notched metallic materials). Accordingly, the proposed simplified design methodology can safely be used in situations of practical interest - by achieving a higher level of accuracy compared to the one obtained by applying the HSSM – provided that appropriate safety factors are adopted. This aspect of the problem will be addressed in the next section.

6. Design safety factors

After assessing the overall accuracy of both the HSSM and the simplified TCD, the next step is to define appropriate values for the safety factors that allow notched components to be designed against static loading by systematically reaching an adequate level of safety.

According to the error values reported in Table 4, the highest level of accuracy was obtained by using σ_1 to assess brittle/quasi-brittle materials and σ_{VM} to assess metallic materials. Thus, the above equivalent stresses together with both the HSSM and the simplified TCD will be used in what follows to determine the corresponding design safety factors.

Table 5 lists the recommended values for S_F calculated according to definition (7) for the simplified TCD and to definition (9) for the HSSM. The calculated safety factors were re-analysed according to the “engineering rule of thumb” (i.e., the "three-standard-deviations rule") [38]. This simplified statistical approach postulates that at least 97.7% of cases should fall within the three standard deviations interval [39]. Therefore, the recommended values for the safety factor (for a probability, P, equal to 97.7%) listed in Table 5 were determined as the calculated mean value plus three times the associated standard deviation.

The diagrams reported in Figure 8 confirm the validity of the assumptions that were made to estimate the S_F values listed in Table 5. These diagrams were built by using the simplified TCD and the HSSM to calculate the safety factors associated with the experimental results summarised in Tables 1 to 3. Figure 8 makes it evident that the proposed values for S_F allow the simplified TCD to be employed in situations of practical interest by always reaching an adequate level of safety and a remarkably lower level of scattering compared to the HSSM. Since the design approach being investigated in the present paper is as simple to apply as the classic HSSM, this result is certainly remarkable. In fact, the higher level of correlation being obtained allows the design boundaries in terms of strength, capacity, operational lifetime, etc. to be pushed while maintaining an appropriate level of safety. In situations of practical interest, this is expected to result in a more efficient usage of materials and energy during manufacturing, with this leading to a remarkable reduction of the production costs.

To conclude, it is worth observing that the safety factors as defined according to Eqs (7) and (9) [38] refer solely to the material UTS. Therefore, they do not take into account the effect of important variables such as: manufacturing defects, imperfections, variation in the properties of the material and its deterioration during in-service operations, type of loading and potential overloadings, etc. Since these aspects can all reduce the strength of notched components significantly, the proposed approach is recommended to be used by increasing the reference values listed in Table 5 via appropriate enhancement factors that take into account the specific needs/characteristics of the notched structural member being designed.

7. Discussion

The simplified engineering method proposed in the present paper is suitable for the design of notched components that experience uniaxial and multiaxial static loading, without the need for expensive testing. In particular, critical distance L_E can directly be estimated according to definition (4), i.e., by using two material properties that are usually available.

According to Figures 6 and 7, the systematic use of the simplified TCD resulted in estimates falling in an error range that was an order of magnitude lower than the one obtained by applying the HSSM. Turning to the recommended values for the design safety factors (Tab. 5), although the S_F values suggested as being used along with the simplified TCD are slightly larger than the ones which should be used with the HSSM, the overall accuracy obtained through the TCD is in any case remarkably higher. Accordingly, the proposed simplified design methodology allows structural engineers to design lighter components and structures, which consume less material and energy to produce yet have the required degree of structural durability.

On the other hand, if the level of conservatism is an important factor such as high performance components where weight and/or size are crucial, it is recommended that the rigorous application of the original TCD be used. In fact, whilst the simplified version of the TCD being proposed here is capable of estimates falling within an error range, ΔE, of about 150% (see Table 4), the systematic use of the original method has been proven to result in predictions falling within an error range of 40% [2-8].

When the proposed simplified approach is used to design real components, attention must be paid to correctly take into account three-dimensional effects and stress states near sharp and rounded notches [40, 41]. In particular, in the vicinity of a stress concentrator the actual linear-elastic stress distribution varies across the thickness, with this holding true both under normal [40, 42, 43] and shear loading [40, 44, 45]. Under these circumstances, the problem is that the maximum value of the local stress is away from the surface [40]. As far as real three-dimensional components are concerned, this results in the fact that a safe design can be performed provided that the required FE models are done so that the adopted mesh is capable of capturing the through-thickness local effects. Accordingly, in the presence of three-dimensional stress concentrators the simplified formulation of the TCD proposed in the present paper has to be applied by considering the maximum sub-surface stress determined either according to the maximum principal stress criterion (for brittle/quasi-brittle materials) or in terms of von Mises' equivalent stress (for ductile materials). In this context, it is worth observing that, recently, this numerical stress analysis technique applied along with the rigorous formulation of the PM was seen to be successful in estimating both static [46] and high-cycle multiaxial fatigue strength [47] of three-dimensional stress raisers.

Finally, it is worth mentioning that predictions made in practical applications may have increased conservatism. This is because engineering values supplied by manufacturers are typically given as minimum values compared to the average test values typically reported in technical literature. From the design engineer point of view this should be seen as a positive factor in achieving a safe design.

8. Conclusions

- The proposed method was validated using approximately 800 test data with many test data representing an average of 3-5 tests per geometry and loading case.

- The use of the simplified TCD results in a much higher level of accuracy than the one obtained by applying the conventional HSSM.
- The proposed simplified methodology is capable of consistently assess both notched and un-notched components.
- The simplified TCD allows notched components to be designed against static loading by directly post-processing the results from conventional linear-elastic FE models, this holding true independently of the mechanical behaviour displayed by the material being assessed.
- To design brittle/quasi-brittle notched materials, the simplified TCD is recommended to be used along with the maximum principal stress criterion by adopting a design safety factor equal to (or larger than) 1.5.
- The simplified TCD applied along with Von Mises' equivalent stress can be used to design notched metallic materials, provided that the design safety factor is taken equal to (or larger than) 2.
- The simplified PM should be used to design components having relevant dimensions at least an order of magnitude larger than engineering critical distance L_E.
- More experimental work needs to be done in this area to investigate the mechanical behaviour of notched metallic materials under uniaxial/multiaxial static loading.

ACKNOWLEDGEMENTS

3DS Dassault Systems (www.3ds.com) is acknowledged for fully supporting the present research investigation.

References

[1] Susmel L, Taylor D. The Theory of Critical Distances to estimate the static strength of notched samples of Al6082 loaded in combined tension and torsion. Part I: Material cracking behaviour. Eng. Fract. Mech. 2010;77:452–469.

[2] Taylor D. The Theory of Critical Distances: A new perspective in fracture mechanics. Elsevier Ltd, Oxford, UK, 2007.

[3] Taylor D. Predicting the fracture strength of ceramic materials using the theory of critical distances. Eng. Fract. Mech.2004;71:2407–2416.

[4] Taylor D, Merlo M, Pegley R, Cavatorta MP. The effect of stress concentrations on the fracture strength of polymethylmethacrylate. Mater. Sci. Engng 2004;A382:288–94.

[5] Taylor D, Cornetti P, Pugno N. The fracture mechanics of finite crack extension. Eng. Frac. Mech. 2005;72:1021-1038.

[6] Susmel L, Taylor D. The Theory of Critical Distances to predict static strength of notched brittle components subjected to mixed-mode loading. Eng. Fract. Mech. 2008;75:534–550.

[7] Susmel L, Taylor D. On the use of the Theory of Critical Distances to predict static failures in ductile metallic materials containing different geometrical features. Eng. Fract. Mech. 2008;75:4410–4421.

[8] Susmel L, Taylor D. The Theory of Critical Distances to estimate the static strength of notched samples of Al6082 loaded in combined tension and torsion. Part II: Multiaxial static assessment. Eng. Fract. Mech. 2010;77:470–478.

[9] Neuber H. Theory of notch stresses: principles for exact calculation of strength with reference to structural form and material. 2nd ed. Berlin: Springer Verlag; 1958.

[10] Peterson RE. Notch sensitivity. In: Sines G, Waisman JL, editors. Metal fatigue. New York, USA: McGraw Hill; 1959. p. 293–306.

[11] Whitney JM, Nuismer RJ. Stress Fracture Criteria for Laminated Composites Containing Stress Concentrations. J. Compos. Mater.1974;8:253–265.

[12] Susmel L. Multiaxial Notch Fatigue: from nominal to local stress-strain quantities. Woodhead & CRC, Cambridge, UK, 2009.

[13] Ameri AAH, Davison JB, Susmel L. On the use of linear-elastic local stresses to design steel arc welded joints against static loading. Eng. Fract. Mech. 2015;136:2015.

[14] Gómez FJ, Elices M, Berto F, Lazzarin P. Local strain energy to assess the static failure of U-notches in plates under mixed mode loading. Int. J. Fract. 2007;145(1): 29–45.

[15] Gómez PFJ; Elices M, Berto F, Lazzarin P. Fracture of V-notched specimens under mixed mode (I + II) loading in brittle materials. Int. J. Fract. 2009;159(2): 121–135.

[16] Gómez FJ, Elices M, Berto F, Lazzarin P. Fracture of U-notched specimens under mixed mode: Experimental results and numerical predictions. Eng. Fract. Mech. 2009;76(2):236–249.

[17] Gómez, FJ, Elices, M, Planas J. The cohesive crack concept: application to PMMA at −60°C. Eng. Fract. Mech. 2005;72(8):1268–1285.

[18] Berto F, Cendon D, Lazzarin P, Elices M. Fracture behaviour of notched round bars made of PMMA subjected to torsion at −60°C. Eng. Fract. Mech. 2013;102:271–287.

[19] Ayatollahi MR, Torabi AR. Tensile fracture in notched polycrystalline graphite specimens. Int. J. Carbon 2010;48(8):2255–2265.

[20] Ayatollahi MR, Torabi AR. Experimental verification of RV-MTS model for fracture in soda-lime glass weakened by a V-notch. J. Mech. Sci. Technol. 2011;25(10):2529–2534.

[21] Yosibash Z, Bussiba A, Gilad I. Failure criteria for brittle elastic materials. Int. J. Fract. 2004;125(1957):307–333, 2004.

[22] Berto F, Lazzarin P, Marangon C. Brittle fracture of U-notched graphite plates under mixed mode loading. Mater. Des. 2012;41: 421–432.

[23] Lazzarin P, Berto F, Ayatollahi MR. Brittle failure of inclined key-hole notches in isostatic graphite under in-plane mixed mode loading. Fatigue Fract. Eng. Mater. Struct. 2013;36(9):942–955.

[24] Gómez FJ, Elices M. Fracture of components with V-shaped notches. Eng. Fract. Mech. 2003;70(14):1913–1927.

[25] Gomez FJ, Elices M, Valiente A. Cracking in PMMA containing U-shaped notches. Fatigue Fract. Eng. Mater. Struct. 2000;23(9):795–803.

[26] Ayatollahi MR, Torabi AR, Azizi P. Experimental and Theoretical Assessment of Brittle Fracture in Engineering Components Containing a Sharp V-Notch. Exp. Mech. 2010;51(6):919–932.

[27] Berto F, Ayatollahi MR. Fracture assessment of Brazilian disc specimens weakened by blunt V-notches under mixed mode loading by means of local energy. Mater. Des. 2011;32(5):2858–2869.

[28] Torabi AR, Amininejad S. Fracture assessment of VO-notches under mode II loading: Experiments and theories. Theor. Appl. Fract. Mech. 2015;75:59-69.

[29] Cicero S, Madrazo V, Carrascal IA. Analysis of notch effect in PMMA using the Theory of Critical Distances. Eng. Fract. Mech. 2012;86:56–72.

[30] Berto F, Elices M, Lazzarin P, Zappalorto M. Fracture behaviour of notched round bars made of PMMA subjected to torsion at room temperature. Eng. Fract. Mech. 2012;90:143–160.

[31] Seweryn A, Poskrobko S, Mroz Z. Brittle fracture in plane elements with sharp notches under mixed-mode loading. J. Engng Mech. ASCE 1997;123(6):535-43.

[32] Shinde PS, Singh KK, Tripathi VP, Sarkar K, Kumar P. Fracture toughness of thin aluminum sheets using modified single edge notch specimen. International Journal of Engineering and Innovative Technology 2012;1(5):283-288.

[33] Gómez FJ, Elices M, Valiente A. Fracture of a high strength steel containing U-notches. In: Proceedings of The 13th International Conference on Fracture (ICF13), 16-21 June 2013, Beijing, China (available at www.gruppofrattura.it).

[34] Taghizadeh K, Berto F, Barati E. Local strain energy density applied to martensitic steel plates weakened by U-notches under mixed mode loading. Theor. Appl. Fract. Mech. 2012;59(1):21–28.

[35] Susmel L, Taylor D. The Theory of Critical Distances to estimate the static strength of notched samples of Al6082 loaded in combined tension and torsion. Part I: Material cracking behaviour. Eng. Fract. Mech. 2010;77: 452–469.

[36] Berto F, Barati E. Fracture assessment of U-notches under three point bending by means of local energy density. Mater. Des. 2011;32(2):822–830.

[38] Beer FP, Johnson ER, De Wolf JT. Mechanics of Materials. McGraw-Hill, New York, USA, 2008.

[39] Pukelsheim F. The Three Sigma Rule. American Statistician (American Statistical Association) 1994;48(2):88–91.

[40] Pook LP. A 50-year retrospective review of tree-dimensional effects at cracks and sharp notches. Fatigue Fract. Engng Meter. Struct. 2013;36:699-723.

[41] Lazzarin P, Zappalorto M. A three-dimensional stress field solution for pointed and sharply radiused V-notches in plates of finite thickness.

[42] Dixon JR. Effects of crack-front geometry and plate thickness on the stress distribution in cracked plates. In: Proc. Conf. Physical Basis of Yield and Fracture (edited by Stickland, AC). Institute of Physics and Physical Society, London, UK, pp. 6-16, 1967.

[43] Meneghetti G, Susmel L, Tovo R. High-Cycle Fatigue Crack Paths in Specimens having Different Stress Concentration Features. Eng. Fail. Anal. 2007;14:656-672.

[44] Berto F, Lazzarin P, Kotousov A, Pook LP. Induced out-of-plane mode at the tip of blunt notches and holes under in-plane shear loading. Fatigue Fract. Engng Meter. Struct. 2012;35:538-555.

[45] Pook LP, Campagnolo A, Berto F. Coupled fracture modes of discs and plates under anti-plane loading and a disc un in-plane shear loading. Fatigue Fract. Engng Meter. Struct. 2016 (in press) DOI: 10.1111/ffe.12389.

[46] Ameri AAH, Davison JB, Susmel L. On the use of linear-elastic local stresses to design load-carrying fillet-welded steel joints against static loading. Eng. Fract. Mech. 2015;136:38-57.

[47] Louks R, Gerin B, Draper J, Askes H, Susmel L. On the multiaxial fatigue assessment of complex three-dimensional stress concentrators. Int. J. Fatigue 2014;63:12-24.

List of captions

Table 1. Summary of the data generated by testing brittle materials.

Table 2. Summary of the data generated by testing quasi-brittle materials.

Table 3. Summary of the data generated by testing metallic materials.

Table 4. Accuracy of the HSSM and the simplified PM in assessing the static strength of the considered materials.

Table 5. Recommended value to use the simplified PM and HSSM in situations of practical interest.

Figure 1. Notched plate loaded in tension and local system of coordinates (a). Effective stress σ_{eff} estimated according to the Point (b) and Line Method (d).

Figure 2. Determination of critical distance L and inherent strength σ_0 via results generated by testing notches of different sharpness.

Figure 3. Orientation of the focus path under multiaxial loading for brittle (a) and ductile materials (b) – the schematic stress-distance curve reported in Figure 3b is assumed to be determined by using a linear-elastic constitutive law to model the mechanical behaviour of the material being assessed.

Figure 4. Simplified reformulation of the PM.

Figure 5. Static assessment of notched ductile materials performed using L_E and L.

Figure 6. Accuracy of the HSSM in estimating static strength of brittle (a), quasi-brittle (b), and ductile (c, d) notched materials (N.B. In Figures 6c and 6d series M1 is not displayed because the associated errors are larger than 1600%).

Figure 7. Accuracy of the simplified PM in estimating static strength of brittle (a), quasi-brittle (b), and metallic (c, d) materials.

Figure 8. Recommended values for the safety factors to design notched components against static loading using the HSSM (a, b) as well as the simplified PM (c, d).

Tables

Code	**Ref.**	**Material**	**Testing Temperature** [° C]	**Load Modes**	**Testing Set-up**[(a)]	K_{IC} [MPa m$^{1/2}$]	σ_{UTS} [MPa]	L_E [mm]	ρ [mm]
B1	[14]	PMMA	-60	I+II	TPB	1.7	128.4	0.056	0.01÷4
B2	[15]	PMMA	-60	I+II	TPB	1.7	128.4	0.056	0.018÷0.072
B3	[16]	PMMA	-60	I+II	TPB	1.7	128.4	0.056	0.01÷4
B4	[17]	PMMA	-60	I	TPB/Te	1.7	128.4	0.056	0.04÷7.07
B5	[18]	PMMA	-60	III	To	1.7	153.1	0.039	0.1÷7
B6	[19]	Polycrystalline Graphite	RT	I	TPB/HBD/BD	1.0	27.5	0.421	1÷4
B7	[20]	Soda-Lime Glass	RT	I, I+II, II	BD	0.6	14.0	0.585	1÷4
B8	[21]	Alumina-7%Zirconia	RT	I	TPB/FPB	8.1	509.0	0.081	0.031÷0.1
B9	[22]	Isostatic Graphite	RT	I, I+II	Te	1.1	46.0	0.169	0.25÷4
B10	[23]	Isostatic Graphite	RT	I, I+II	Te	1.1	46.0	0.169	0.25÷4

(a)TPB = Three Point Bending; FPB = Four Point Bendig; Te = Tension; To = Torsion; BD = Brazilian disk; HBD = Brazilian disk

Table 1. Summary of the data generated by testing brittle materials.

Code	Ref.	Material	Testing Temperature [° C]	Load Modes	Testing Set-up[(a)]	K_{IC} [$MPa\ m^{1/2}$]	σ_{UTS} [MPa]	L_E [mm]	ρ [mm]
QB1	[24]	PMMA	RT	I	TPB	1.0	75.0	0.057	0.08
QB2	[25]	PMMA	RT	I	TPB	1.0	75.0	0.057	0.1÷4
QB3	[26]	PMMA	RT	I, I+II, II	BD	2.0	70.5	0.246	0.05÷0.07
QB4	[27]	PMMA	RT	I, I+II, II	BD	2.0	70.5	0.246	1÷4
QB5	[28]	PMMA	RT	I, II	BD	1.0	75.0	0.057	0.5÷4
QB6	[6]	PMMA	RT	I, I+III, III	Te/To	2.2	67.0	0.343	0.2÷4
QB7	[29]	PMMA	RT	I	TPB	2.0	72.0	0.253	0.1÷2.5
QB8	[30]	PMMA	RT	III	To	1.0	67.0	0.071	0.1÷7
QB9	[31]	PMMA	RT	I, I+II, II	Te	1.4	115.0	0.045	0.01

(a)TPB = Three Point Bending; Te = Tension; To = Torsion; BD = Brazilian disk

Table 2. Summary of the data generated by testing quasi-brittle materials.

Code	Ref.	Material	Testing Temperature [° C]	Load Modes	Testing Set-up	K_{IC} [$MPa\ m^{1/2}$]	σ_{UTS} [MPa]	L_E [mm]	ρ [mm]
M1	[32]	Aluminium Alloy 6061	RT	I	Te	25.0	319.8	1.945	0.012
M2	[33]	High Strength Steel	RT	I	TPB	33.0	1285.0	0.210	0.1÷1
M3	[7]	En3B	RT	I	TPB	97.4	638.5	7.400	0.1÷5
M4	[34]	Martensitic Tool Steel	RT	I+II	TPB	6.1	1482.0	0.005	0.2÷2
M5	[35]	Aluminium Alloy 6082	RT	I, I+III, III	Te/To	31.1	367.0	2.286	0.44÷4
M6	[36]	Al-15%SiC	RT	I	TPB	6.0	230.0	0.217	0.5÷2
M7	[36]	Ferritic–Pearlitic Steel	-40	I	TPB	12.3	502.0	0.191	0.5÷1.5

(a)TPB = Three Point Bending; Te = Tension; To = Torsion

Table 3. Summary of the data generated by testing metallic materials.

Design Methodology	Error[(a)] [%]											
	Brittle Materials				Quasi-Brittle Materials				Metallic Materials			
	E_{max}	E_{min}	E_a	ΔE	E_{max}	E_{min}	E_a	ΔE	E_{max}	E_{min}	E_a	ΔE
HSSM with $\sigma_{HS,eq}=\sigma_1$	915	-33	111	948	1588	-39	171	1627	4329	-6	488	4335
HSSM with $\sigma_{HS,eq}=\sigma_{VM}$	-	-	-	-	-	-	-	-	3699	-11	441	3710
PM with $\sigma_{eq}=\sigma_1$	193	-33	32	161	116	-53	18	169	306	-70	12	376
PM with $\sigma_{eq}=\sigma_{VM}$	-	-	-	-	-	-	-	-	91	-49	-13	140

[(a)] E_{max}=maximum error; E_{min}=minimum error; E_a=average error; ΔE=error range ($\Delta E=E_{max}-E_{min}$)

Table 4. Accuracy of the HSSM and the simplified PM in assessing the static strength of the considered materials.

Methodology	Safety Factor, S_F					
	Brittle/Quasi-Brittle Materials			Metallic Materials		
	Mean	Standard Deviation	P=97.7%	Mean	Standard Deviation	P=97.7%
HSSM with $\sigma_{HS,eq}=\sigma_1$	0.6	0.3	1.4	-	-	-
HSSM with $\sigma_{HS,eq}=\sigma_{VM}$	-	-	-	0.6	0.3	1.6
PM with $\sigma_{eq}=\sigma_1$	0.9	0.2	1.5	-	-	-
PM with $\sigma_{eq}=\sigma_{VM}$	-	-	-	1.2	0.25	2.0

Table 5. Recommended value to use the simplified PM and HSSM in situations of practical interest.

Figures

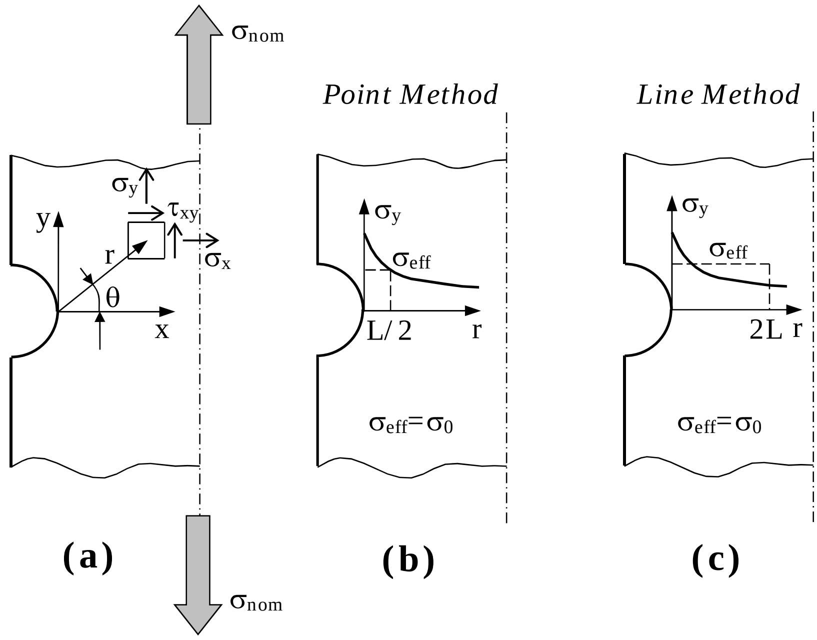

Figure 1. Notched plate loaded in tension and local system of coordinates (a). Effective stress σ_{eff} estimated according to the Point (b) and Line Method (d).

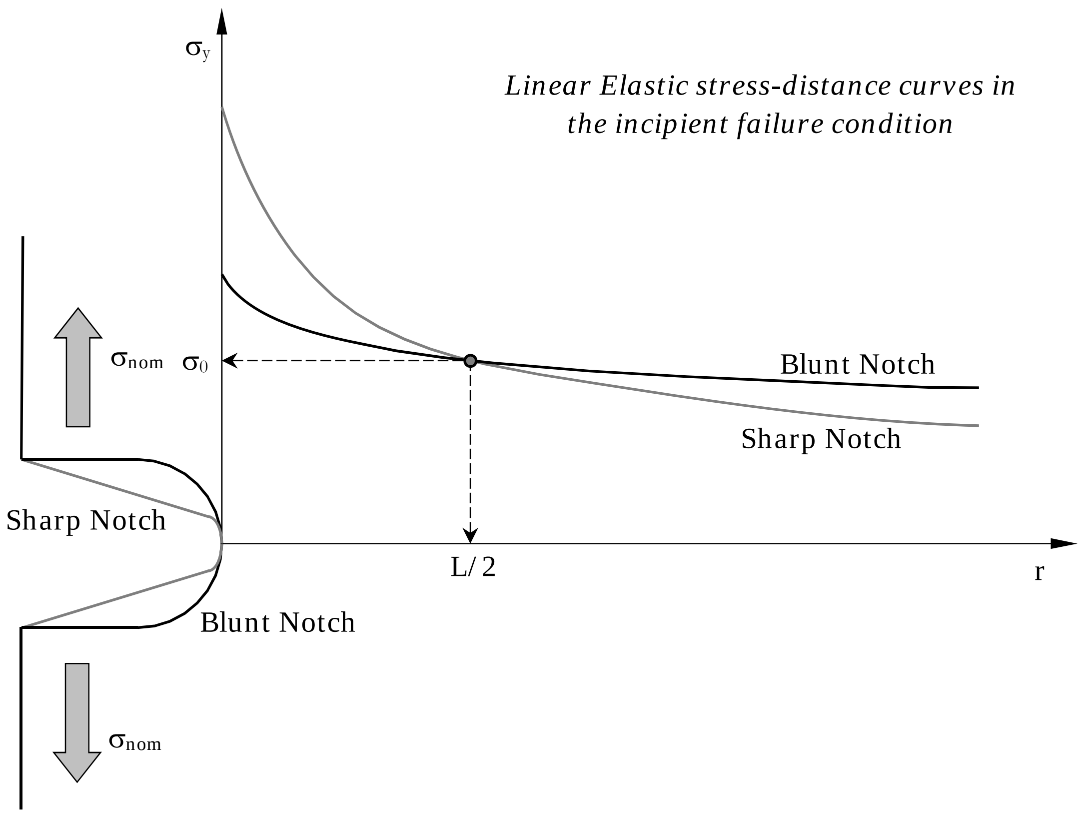

Figure 2. Determination of critical distance L and inherent strength σ_0 via results generated by testing notches of different sharpness.

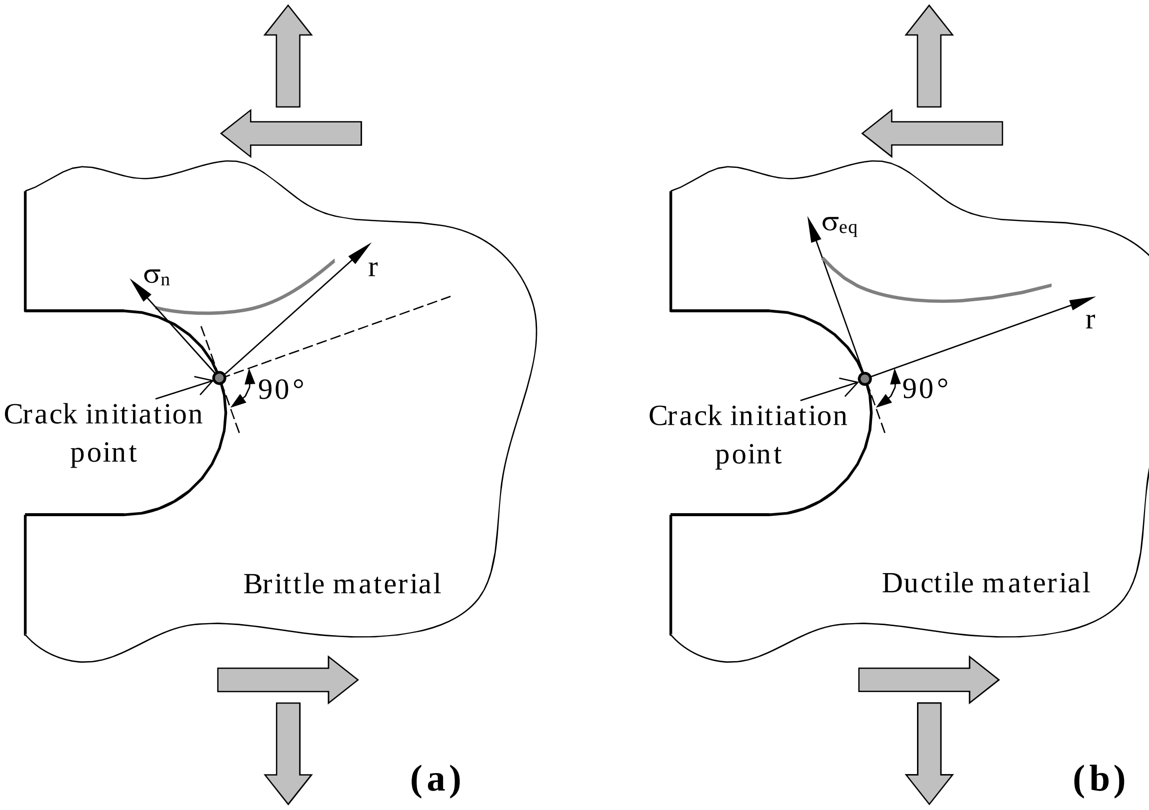

Figure 3. Orientation of the focus path under multiaxial loading for brittle (a) and ductile materials (b) – the schematic stress-distance curve reported in Figure 3b is assumed to be determined by using a linear-elastic constitutive law to model the mechanical behaviour of the material being assessed.

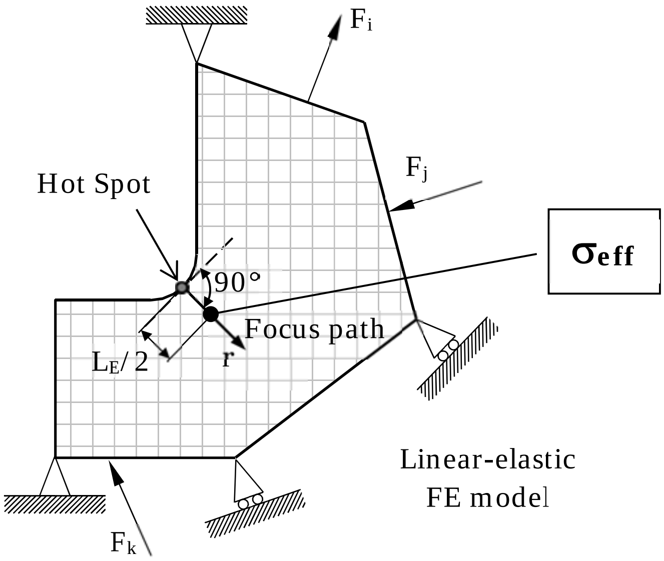

Figure 4. Simplified reformulation of the PM.

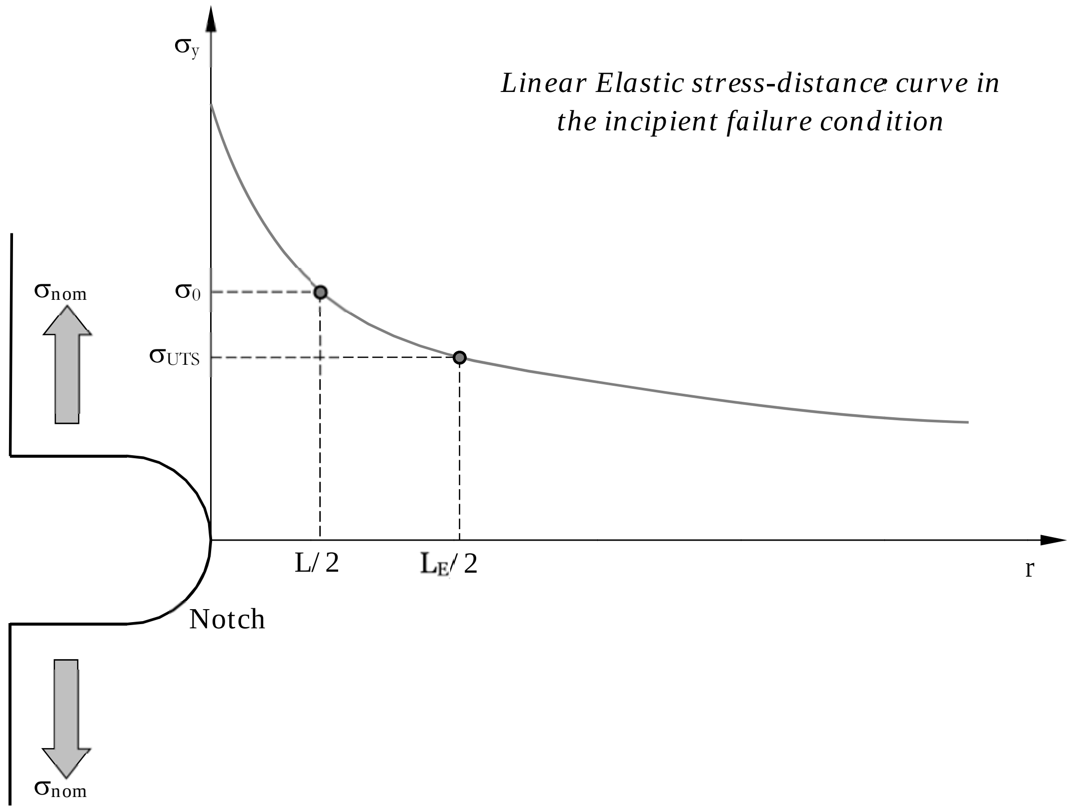

Figure 5. Static assessment of notched ductile materials performed using L_E and L.

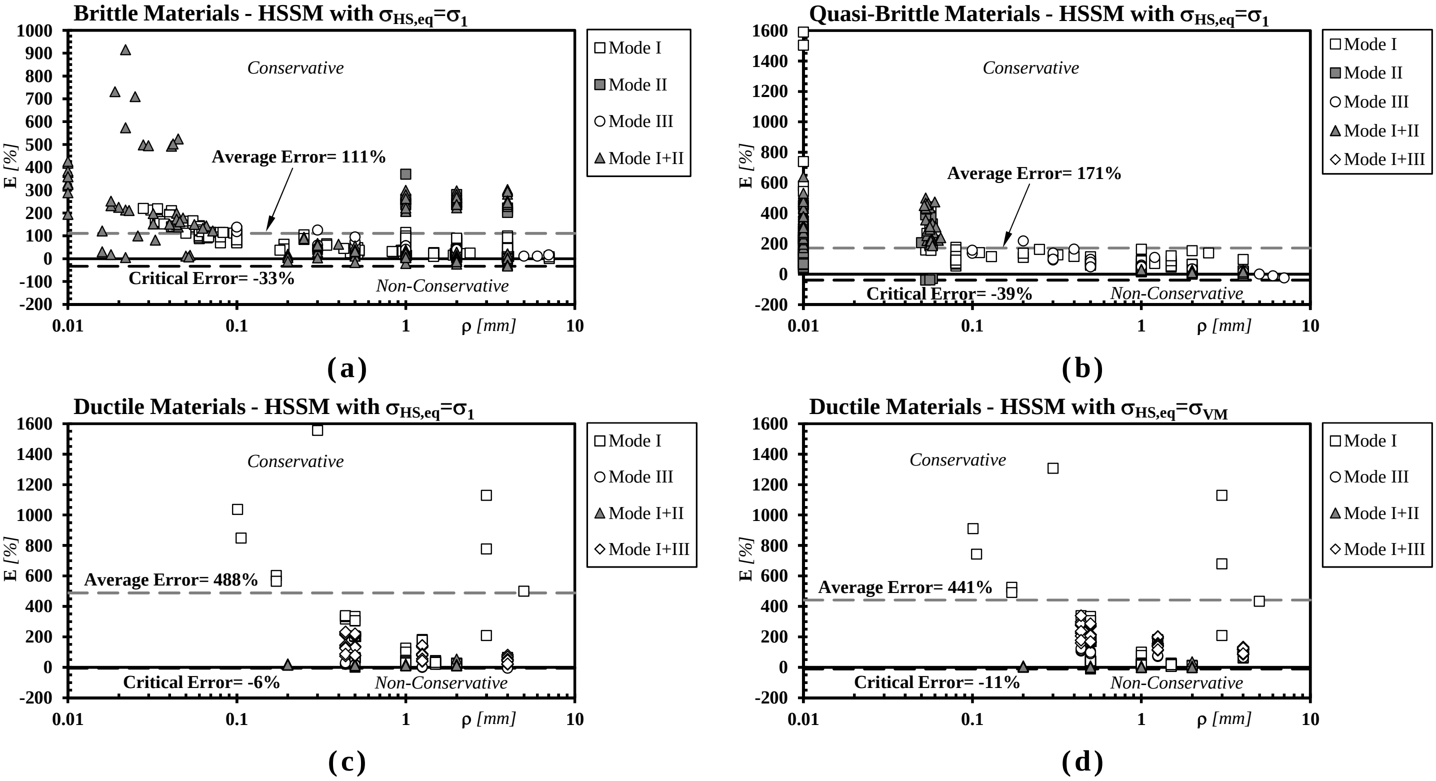

Figure 6. Accuracy of the HSSM in estimating static strength of brittle (a), quasi-brittle (b), and ductile (c, d) notched materials (N.B. In Figures 6c and 6d series M1 is not displayed because the associated errors are larger than 1600%).

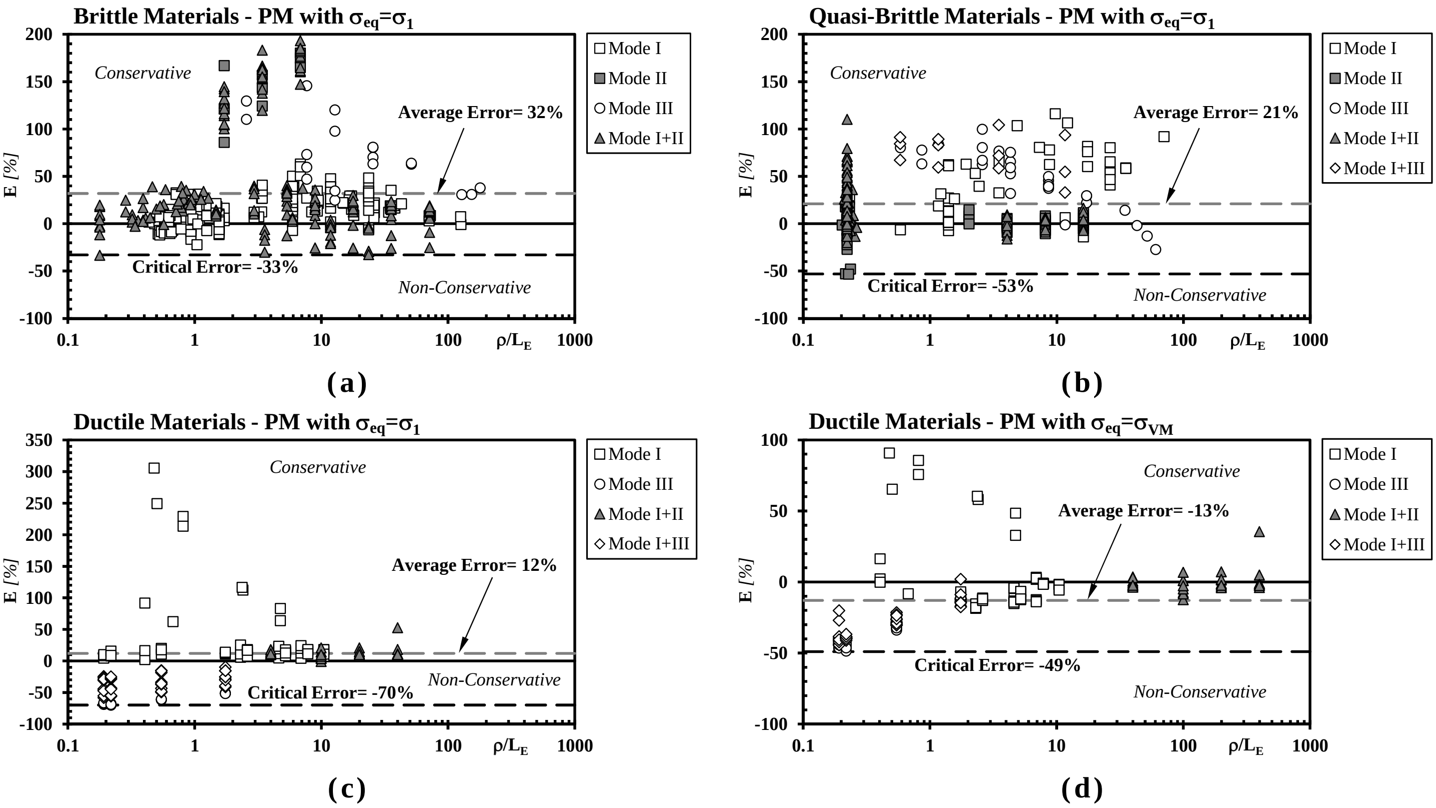

Figure 7. Accuracy of the simplified PM in estimating static strength of brittle (a), quasi-brittle (b), and metallic (c, d) materials.

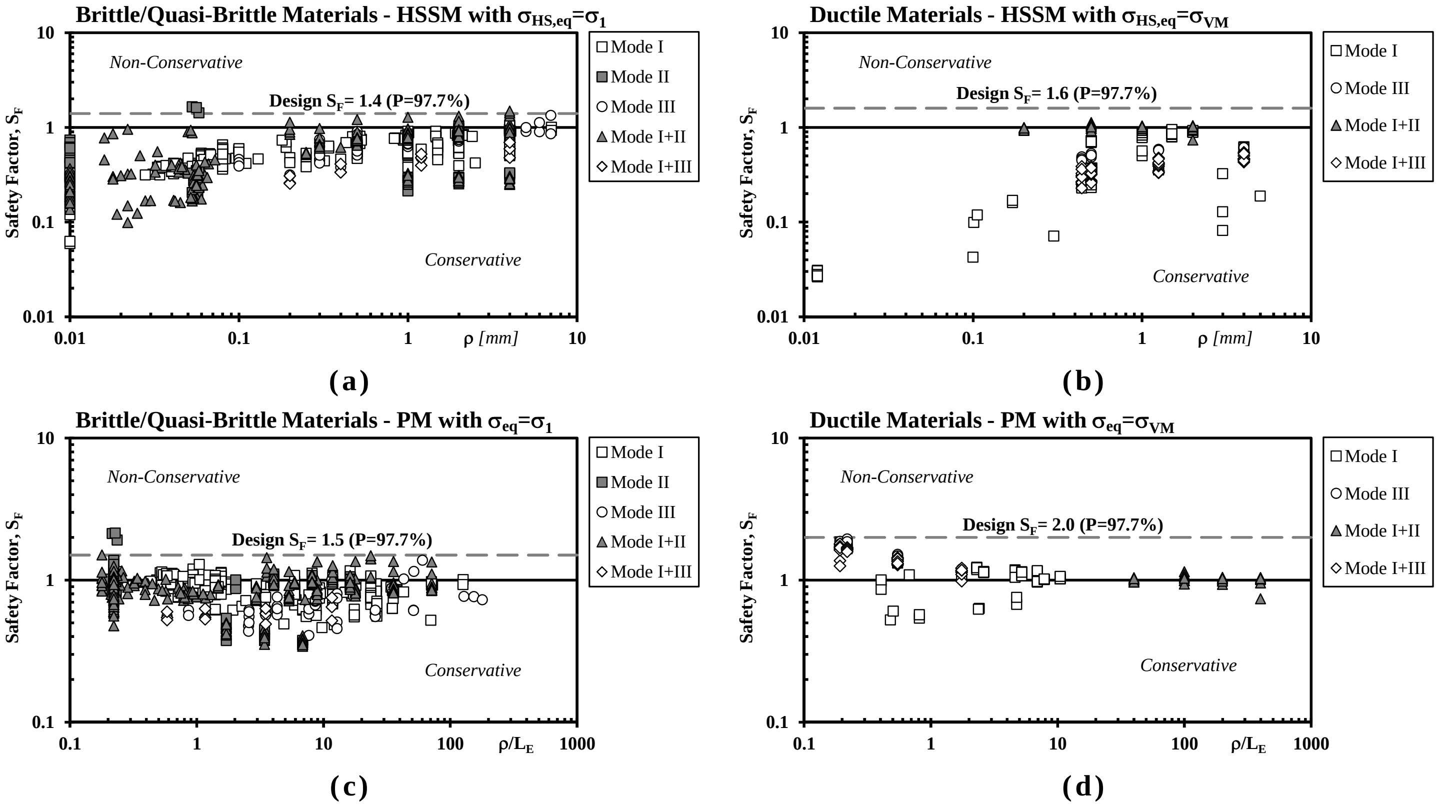

Figure 8. Recommended values for the safety factors to design notched components against static loading using the HSSM (a, b) as well as the simplified PM (c, d).